



HAL
open science

Artifacts in magnetic force microscopy under in-plane applied magnetic field: Magnetic bubble as a case study

Ibrahim Cinar, Daniel Lacour, François Montaigne, Vito Puliafito, Sébastien Petit, Michel Hehn, Giovanni Finocchio, Ozhan Ozatay, Thomas Hauet

► To cite this version:

Ibrahim Cinar, Daniel Lacour, François Montaigne, Vito Puliafito, Sébastien Petit, et al.. Artifacts in magnetic force microscopy under in-plane applied magnetic field: Magnetic bubble as a case study. *Journal of Magnetism and Magnetic Materials*, 2020, 500, pp.166296. 10.1016/j.jmmm.2019.166296 . hal-02901555

HAL Id: hal-02901555

<https://hal.science/hal-02901555v1>

Submitted on 27 Sep 2020

HAL is a multi-disciplinary open access archive for the deposit and dissemination of scientific research documents, whether they are published or not. The documents may come from teaching and research institutions in France or abroad, or from public or private research centers.

L'archive ouverte pluridisciplinaire **HAL**, est destinée au dépôt et à la diffusion de documents scientifiques de niveau recherche, publiés ou non, émanant des établissements d'enseignement et de recherche français ou étrangers, des laboratoires publics ou privés.

Artifacts in magnetic force microscopy under in-plane applied magnetic field: Magnetic bubble as a case study

Ibrahim Cinar^{a,b,*}, Daniel Lacour^b, Francois Montaigne^b, Vito Puliafito^c, Sebastien Petit Watelot^b, Michel Hehn^b, Giovanni Finocchio^d, Ozhan Ozatay^e, Thomas Hauet^b

^a Department of Medical Services and Techniques, Karamanoglu Mehmetbey University, 70100 Karaman, Turkey

^b Institut Jean Lamour, UMR CNRS-Université de Lorraine, 54011 Nancy, France

^c Department of Engineering, University of Messina, Messina, Italy

^d Department of Mathematical and Computer Sciences, Physical Sciences and Earth Sciences, University of Messina, Messina, Italy

^e Department of Physics, Bogazici University, 34342 Bebek, Istanbul, Turkey

The study of magnetic bubble configuration in Co/Ni multilayers circular dots under in-plane magnetic field enlightens two magnetic force microscopy (MFM) measurement artifacts. We demonstrate that any tilt of the magnetic field producing out-of-plane field component due to the inhomogeneity of the MFM set up strongly affects the shape and size of the magnetic bubble independently of the in-plane field component intensity. Furthermore, MFM signal variations for in-plane magnetic field larger than 0.1 Tesla can only be understood considering MFM tip magnetization rotation. These two artifacts can have strong impact on MFM images and need to be carefully checked for reliable results in imaging skyrmionic structures with MFM under-field.

1. Introduction

Magnetic Force Microscopy (MFM) is considered as an effective method for imaging magnetic configurations in thin films with not only in-plane, but also perpendicular magnetic anisotropy with high resolution [1–4]. However this powerful technique is not artifact free. In addition to standard artifacts encountered when performing atomic force microscopy [5] a very common one is the sample-tip interaction which can lead to modification of the observed magnetic configuration [6]. Electrostatic force acting at long range as well as the magnetic force can lead to MFM image misinterpretations [7]. Consequently, it is only when having all the possible artifacts in mind that one can conduct a solid analysis of the acquired MFM images.

Magnetic skyrmionic structures are among the most exciting magnetic objects under research subject nowadays. MFM is a very useful tool to observe these kinds of interesting magnetic configurations. Magnetic bubbles are also one of them. Only few studies about magnetic bubbles hosted by circular dots can be found in the literature. Ref. [8] provides some theoretical stability calculations, while more recently skyrmionic type magnetic configurations behavior under external perpendicular magnetic field were experimentally studied [9,10].

Generally, MFM is used to image magnetic domains in the absence of an external magnetic field. However, it has also proven to be a

powerful tool for imaging of magnetic domains in the presence of an external magnetic field [11,12]. In this study, we have used MFM with in-plane external magnetic field to observe magnetic bubble behavior in Ta (50 Å)/Pt(100 Å)/[Co(2 Å)/Ni(6 Å)]₈/Co(2 Å)/Pt (50 Å) thin film patterned circular dots. We used [Co/Ni] multilayer in our study because it has very well controlled intrinsic magnetic properties [13–17] with limited damping, high perpendicular anisotropy, high spin-polarization and moderate magnetization. In our previous study, nucleation and stability of magnetic bubble was shown in an assembly of patterned dots [17].

Here MFM measurements show that, even in the presence of a large in-plane (IP) external magnetic field, any slightest out-of-plane (OOP) magnetic field component affects the bubble shape and size. Moreover, we observed tip magnetization rotation from out-of-plane to in-plane while applying in-plane magnetic field. We discuss the impact of such tip magnetization rotation on the MFM image.

2. Experimental procedure

We study here a multilayer made of cobalt (Co) and Nickel (Ni) layers with 8 repetitions Ta (50 Å)/Pt(100 Å)/[Co(2 Å)/Ni(6 Å)]₈/Co (2 Å)/Pt(50 Å). The multilayer was deposited using an AJA magnetron sputtering system on thermally oxidized Si (100 nm SiO₂) wafers at

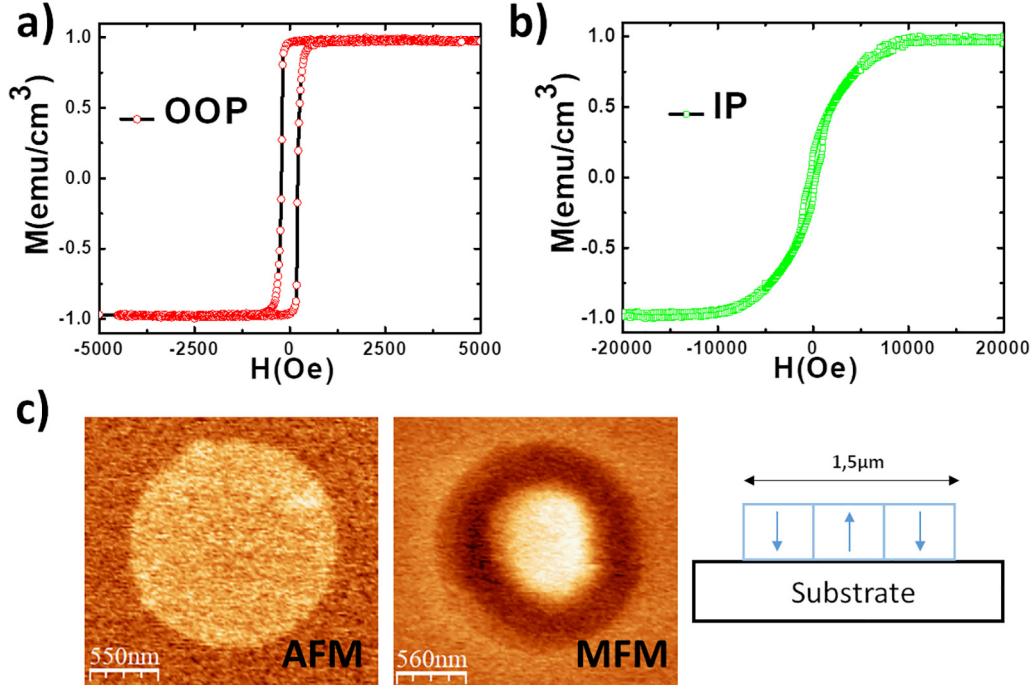


Fig. 1. Co/Ni thin film magnetization versus magnetic field measured by VSM under 0.5T out-of-plane field (a) and 2T in-plane field (b) respectively. (c) AFM and MFM images of 1.5 μm diameter Co/Ni circular dot after AC in-plane external field demagnetization.

room temperature. During deposition, the substrate was rotated for uniformity at about 1.5 Hz. Co was sputtered at 50 W with a deposition rate of 0.23 $\text{\AA}/\text{sec}$ and Ni was sputtered at 50 W with a deposition rate of 0.28 $\text{\AA}/\text{sec}$ using an Argon pressure of 5 mTorr. The multilayer was grown on top of a 50 \AA Ta and 100 \AA Pt buffer layers to get (1 1 1) texture, and covered by a 50 \AA Pt capping layer to prevent oxidation. [Co/Ni] film was patterned to circular dots, with diameters ranging from 1.5 μm , by combining electron beam lithography and ion beam etching. The distance between dots (center-to-center) was set to be four times their diameter in order to have negligible dipolar interactions.

The magnetic properties of the full films at room temperature were determined by using Vibrating Sample Magnetometer (VSM), on a Quantum Design physical properties measurement system (PPMS). Magnetic domain patterns were observed using Magnetic Force Microscopy (MFM), on an Asylum research AFM, MFP-3D Infinity instrument. For MFM imaging, we used Bruker low moment (LM) MESP tips to avoid artifacts due to tip/sample interaction.

3. Results and discussion

Co/Ni thin film sample magnetization loops versus in-plane and out-of-plane magnetic field for our sample are shown in Fig. 1(a) and (b). Saturation magnetization is measured to be $820 \pm 20 \text{ kA/m}$. Moreover, our thin film exhibits a clear perpendicular magnetic anisotropy. The anisotropy constant is obtained from the hard axis in-plane loop as $6.9 \pm 0.1 \cdot 10^5 \text{ J/m}^3$.

Atomic force microscopy (Fig. 1(c)) image indicates that the patterned dot has well defined circular shape. Bubble stabilization in the dot array is achieved through AC in-plane field demagnetization, where the maximum field H_{max} can be adjusted to optimize the bubble nucleation statistics as shown in our previous work [17]. Besides H_{max} , dot diameter is another factor affecting bubble nucleation and stability in a patterned dot array [17]. Fig. 1(c) shows stable magnetic bubble for 1.5 μm diameter patterned dot in 2D and its magnetization direction.

Fig. 2a–f show MFM images of one dot hosting a single magnetic bubble under in-plane magnetic field whose amplitude ranges from zero to 240 Oe. One MFM image was taken every 15 Oe increment. The bubble is found to shrink as the in-plane magnetic field increases. The

diameter of the bubble is around 800 nm at the beginning and after applying 236 Oe, the diameter of bubble is around 600 nm. Also, the bubble wall motion is anisotropic. The same procedure was conducted for different dots among the same array of dots and with the same initial demagnetization process.

In Fig. 3a–f, another sample is shown with in-plane magnetic field values ranging from zero to 609 Oe. Here, surprisingly, we observed enlargement of magnetic bubble (instead of shrinking) when the field amplitude increases. Bubble area at 609 Oe is nearly twice the one at zero field.

The difference in the behavior of the two samples can be understood (i.e. enlarging or shrinking bubble with in plane external magnetic field), by considering the dot position where the applied field direction is not exactly the same as one would assume in the experiments for all samples. It is easy to see this in the MFM set up schematic in Fig. 4. Depending on sample position, the applied magnetic field has both IP and/or OOP magnetic field components, In Fig. 4, region 1 and 2 have opposite perpendicular magnetic field components. Therefore in case 1, bubble shrinks whereas, in case 2, bubble expands. From the experiment under just perpendicular magnetic field, magnetic bubble is affected easily under OOP applied magnetic field and around 60 Oe (there is sample to sample variations like for some samples 50 Oe and for some 75 Oe) is enough for destroying the bubble (annihilating or enlarging and then becoming single domain in disk). Such low depinning field as compared to 210 Oe coercivity field in Fig. 1(a) is linked to the fact that bubble stability here only comes from the stray field in the dot. It does not originate from local strong anisotropy defect which could act as pinning center. Therefore an OOP field as small as 60 Oe is able to overpass the stabilizing stray field.

For instance in the experiment described in Fig. 4, when considering a magnetic field tilt of 2° with respect to the sample plan, an OOP component of 20 Oe/7 Oe is present for an IP measured magnetic field equal to 600 Oe/200 Oe. Such values are high enough to enlarge or reduce the bubble size depending on the dot position with respect to pole pieces (see Fig. 4.). The sign of the OOP magnetic field can even change depending on these positions (e.g. see region 1 and 2 in Fig. 4) leading either to a bubble expansion or reduction as observed in Figs. 2

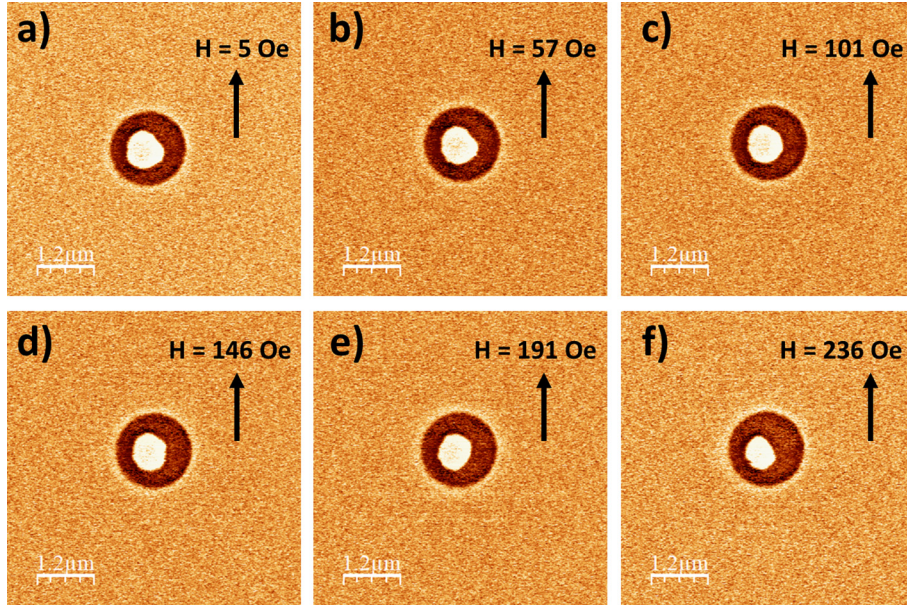


Fig. 2. MFM images of magnetic bubble in a dot for different in-plane external magnetic field values.

and 3.

MFM images of the same dot as in Fig. 3 are presented in Fig. 5 for IP field intensities larger than 600 Oe. At 980 Oe, MFM contrasts changed suddenly. For magnetic fields below this threshold value the MFM contrasts associated with the bubble edges consist of a white ring directly surrounded by a dark one. Beyond the threshold value the bubble edge signature is associated with a contrast having a dark top part and white down part.

One could think that such a change is related to a uniform tilt of the dot magnetization. But, first, the transition is abrupt (less than 15 Oe). Second the MFM pattern due to a moment tilting inside the bubble and the outer region would not fit with the observed MFM signal. On the contrary, as demonstrated below, a switch of tip magnetization from OOP to IP direction induced by the applied magnetic field is consistent with the observed MFM signal change.

In the following we determined the expected MFM phase signal from a bubble in an extended film, considering an MFM tip magnetized

either IP or OOP. To do so, we calculated the derivative of the magnetic force between tip and sample, which we normalized by the magnetic moment of the tip (m_{tip}):

$$\frac{1}{m_{tip}} \frac{\partial F_{mag}}{\partial z} = \cos(\theta) \frac{\partial^2 H_y}{\partial z^2} + \sin(\theta) \frac{\partial^2 H_z}{\partial z^2} \quad (1)$$

H_y and H_z are the magnetic stray field components in the y direction (applied field direction) and z direction (direction perpendicular to the sample plane) and θ is the angle of m_{tip} with respect to y.

According to previous studies our bubble edges are Bloch walls [17,18]. The y and z stray field components can be calculated from the following equations [19] using an $\arctan(y/w)$ domain wall profile:

$$H_z(y, z) = 4M_s \arctan\left(\frac{xh}{(z+w)(z+w+h) + x^2}\right) \quad (2)$$

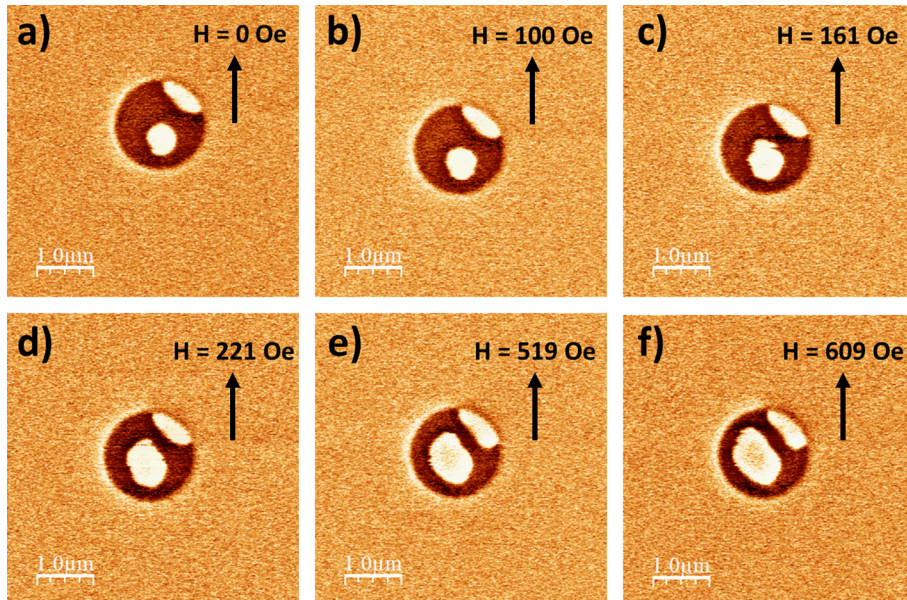


Fig. 3. MFM images of magnetic bubble in a dot for different in-plane external magnetic field values.

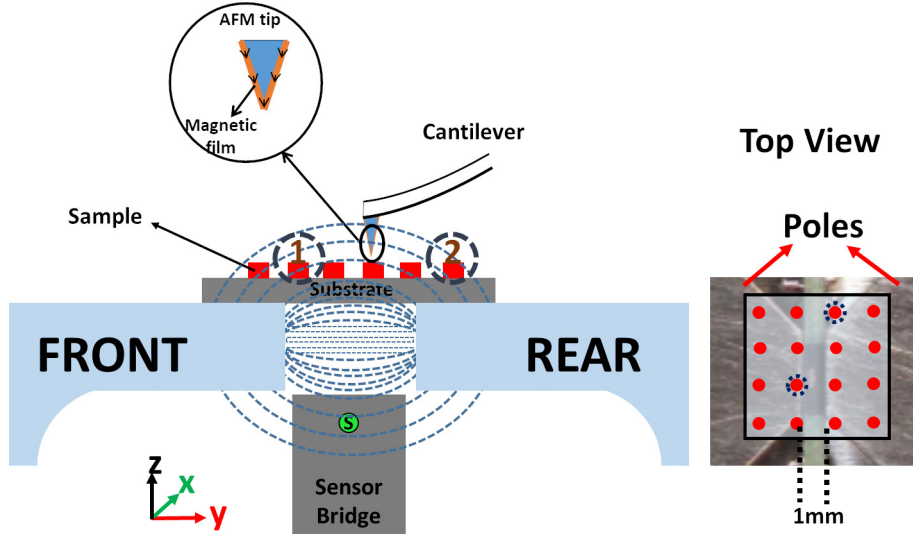


Fig. 4. Schematic illustrations of MFM measurement system from side view and top view. The pole pieces are represented in clear blue. Dot diameter is 1 μm . (For interpretation of the references to colour in this figure legend, the reader is referred to the web version of this article.)

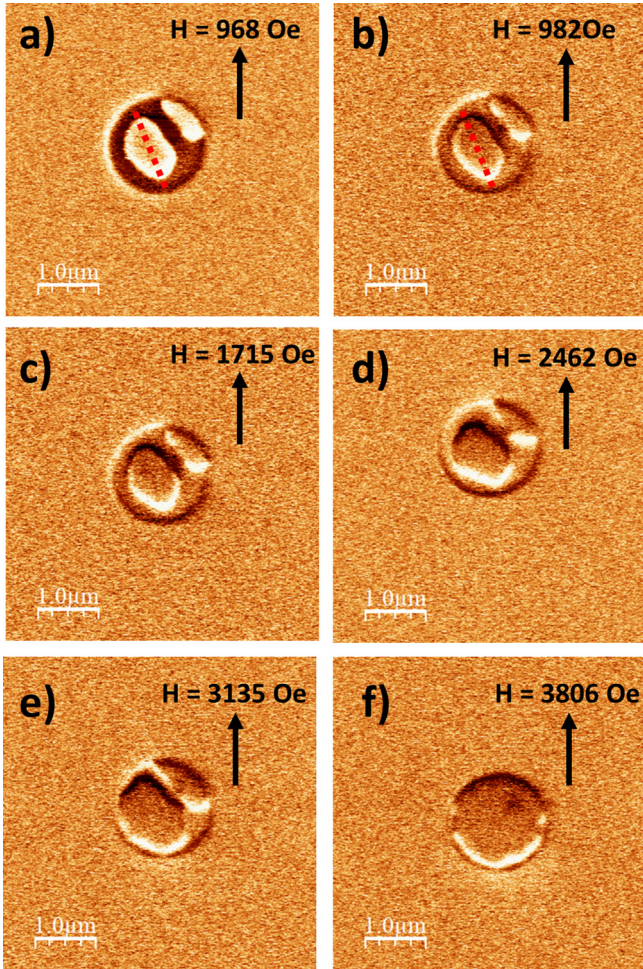


Fig. 5. MFM images of magnetic bubble in a dot for different in-plane external magnetic field values.

$$H_y(y, z) = 2M_s \ln \left(\frac{(z+w+h)^2 + x^2}{(z+w)^2 + x^2} \right) \quad (3)$$

where h is the thickness of sample, w the DW width, and M_s saturation magnetization, and z the distance over the surface. Substituting Eqs. (2)

and (3) in Eq. (1) allows to compute the expected MFM contrast in the two cases of interest.

Results from this computation for the OOP and IP magnetized tip respectively as well as experimental MFM profiles extracted from Fig. 5a) and b) are reported in Fig. 6a) and b). Both experimental profiles are well reproduced by the numerical calculations. This demonstrates that the recorded abrupt change of the MFM signal is consistently explained by a switch of the tip magnetization from OOP to IP.

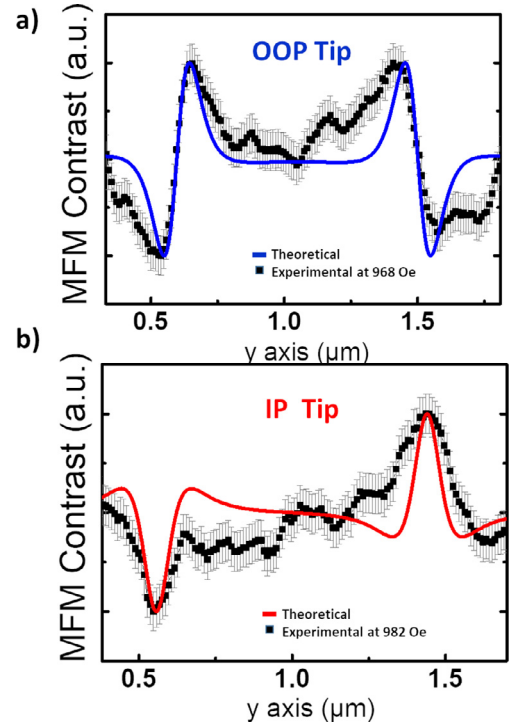


Fig. 6. Calculated MFM signals of magnetic bubble and experimental results for out of plane a) at 968 Oe in Fig. 5a) and in plane b) at 982 Oe in Fig. 5b). The results presented are obtained from a fit using with $h = 28$ nm, $w = 60$ nm as free parameters. The M_s value was taken from measurements presented earlier while the distance z over the surface was fixed to 30 nm during our measurements.

4. Conclusion

We performed MFM measurements under applied magnetic field on magnetic bubbles hosted by circular dots. First, both an increase and decrease of the bubble sizes depending on sample position is reported. Such behavior is attributed to a measurement artifact due to slight misalignment of the magnetic field with respect to sample surface. At higher magnetic field, we record a drastic change of the MFM contrast associated with the bubble edges. This second observation of the bubble is attributed to a switch of the tip magnetization as verified with numerical calculations. These two measurement artifacts should be taken into account when performing magnetic force microscopy under applied magnetic field.

Declaration of Competing Interest

The authors declare that they have no known competing financial interests or personal relationships that could have appeared to influence the work reported in this paper.

Acknowledgments

This work was supported by TUBITAK (Grant No: 114F318) and TUBITAK-BİDEB 2214/A Grant.

References

- [1] U. Hartman, Magnetic force microscopy, *Annu. Rev. Mater. Sci.* 29 (1999) 53–87.
- [2] M.S. Pierce, J.E. Davies, J.J. Turner, K. Chesnel, E.E. Fullerton, J. Nam, R. Hailstone, S.D. Kevan, J.B. Kortright, Kai Liu, L.B. Sorensen, B.R. York, O. Hellwig, Influence of structural disorder on magnetic domain formation in perpendicular anisotropy thin films, *Phys. Rev. B* 87 (2013) 184428.
- [3] Gabriel Bochi, H.J. Hug, D.I. Paul, B. Stiefel, A. Moser, I. Parashikov, H.-J. Güntherodt, R.C. O’Handley, Magnetic domain structure in ultrathin films, *Phys. Rev. Lett.* 75 (1995) 1839.
- [4] V. Gehanno, A. Marty, B. Gilles, Y. Samson, Magnetic domains in epitaxial ordered FePd(001) thin films with perpendicular magnetic anisotropy, *Phys. Rev. B* 55 (1997) 12552.
- [5] Atomic Force Microscopy: Edition 2, Bert Voigtländer May 23, 2019 Springer.
- [6] G. Ciuta, Frédéric Dumas-Bouchiat, Nora Dempsey, Olivier Fruchart, Some aspects of magnetic force microscopy of hard magnetic films, *IEEE Trans. Magn.* 52 (9) (2016) 6500408.
- [7] Livia Angeloni, Daniele Passeri, Melania Reggente, Diego Mantovani, Marco Rossi, Removal of electrostatic artifacts in magnetic force microscopy by controlled magnetization of the tip: application to superparamagnetic nanoparticles, *Sci. Rep.* 6 (2016) 26293.
- [8] C. Moutafis, S. Komineas, C.A.F. Vaz, J.A.C. Bland, T. Shima, T. Seki, K. Takahashi, Magnetic bubbles in FePt nanodots with perpendicular anisotropy, *Phys. Rev. B* 76 (2007) 104426.
- [9] Olivier Bouille, Jan Vogel, Hongxin Yang, Stefania Pizzini, Dayane de Souza, Andrea Locatelli Chaves, Tefvik Onur Menteş, Alessandro Sala, Liliana D. Buda-Prejbeanu, Olivier Klein, Mohamed Belmuguenai, Yves Roussigné, Andrey Stashkevich, Salim Mourad Chérif, Lucia Aballe, Michael Foerster, Mairbek Chshiev, Stéphane Auffret, Ioan Mihai Miron, Gilles Gaudin, Room-temperature chiral magnetic skyrmions in ultrathin magnetic nanostructures, *Nat. Nanotechnol.* 11 (2016) 449–454.
- [10] Yu. Xiuzhen, Yusuke Tokunaga, Yasujiro Taguchi, Yoshinori Tokura, Variation of topology in magnetic bubbles in a colossal magnetoresistive manganite, *Adv. Mater.* 29 (2017) 1603958.
- [11] C. Bran, A. Butenko, N. Kiselev, U. Wolff, L. Schultz, O. Hellwig, U.K. Rößler, A.N. Bogdanov, V. Neu, Evolution of stripe and bubble domains in anti-ferromagnetically coupled [(Co/Pt)8/Co/Ru]18 multilayers, *Phys. Rev. B* 79 (2009) 024430.
- [12] M. Ghidini, G. Zangari, I.L. Prejbeanu, G. Pattanaik, L.D. Buda-Prejbeanu, G. Asti, C. Pernechele, M. Solz, Magnetization processes in hard Co-rich Co-Pt films with perpendicular anisotropy, *J. Appl. Phys.* 100 (2006) 103911.
- [13] S. Girod, M. Gottwald, S. Andrieu, J. McCord, S. Mangin, E. Fullerton, J.M.L. Beaujour, B.J. Krishnatreya, A.D. Kent, Strong perpendicular magnetic anisotropy in Ni/Co(111) single crystal superlattices, *Appl. Phys. Lett.* 94 (2009) 262504.
- [14] S. Mangin, Y. Henry, D. Ravelosona, J.A. Katine, Eric E. Fullerton, Reducing the critical current for spin-transfer switching of perpendicularly magnetized nanomagnets, *Appl. Phys. Lett.* 94 (2009) 012502.
- [15] D.P. Bernstein, B. Brauer, R. Kukreja, J. Stohr, T. Hauet, J. Cucchiera, S. Mangin, J.A. Katine, T. Tyliczszak, K.W. Chou, Y. Acremann, Nonuniform switching of the perpendicular magnetization in a spin-torque-driven magnetic nanopillar, *Phys. Rev. B* (R) 83 (2011) 180410.
- [16] F. Gimbert, L. Calmels, S. Andrieu, Localized electron states and spin polarization in Co/Ni(111) overlayers, *Phys. Rev. B* 84 (2011) 094432.
- [17] T. Liu, V. Puliafito, F. Montaigne, S. Petit, C. Deranlot, S. Andrieu, O. Ozatay, G. Finocchio, T. Hauet, Reproducible formation of single magnetic bubbles in an array of patterned dots, *J. Phys. D Appl. Phys.* 49 (2016) 245002.
- [18] S. Le Gall, N. Vernier, F. Montaigne, A. Thiaville, J. Sampaio, D. Ravelosona, S. Mangin, S. Andrieu, T. Hauet, Effect of spin transfer torque on domain wall motion regimes in [Co/Ni] superlattice wires, *Phys. Rev. B* 95 (2017) 184419.
- [19] M. Gottwald, M. Hehn, D. Lacour, T. Hauet, F. Montaigne, S. Mangin, P. Fischer, M.-Y. Im, A. Berger, Asymmetric magnetization reversal in dipolarly coupled spin valve structures with perpendicular magnetic anisotropy, *Phys. Rev. B* 85 (2012) 064403.